

Feature Clustering to Measure Clutter in Electronic Displays

Maura C. Lohrenz, Geary J. Layne, Stephanie S. Edwards,
Marlin L. Gendron, Jerome T. Bradley
Naval Research Laboratory Code 7440.1
Stennis Space Center, MS 39529

ABSTRACT

A technique is presented to cluster geospatial features on an electronic display and determine a meaningful measure of display clutter. An algorithm previously developed by the Naval Research Laboratory (NRL) to cluster objects in sidescan imagery has been modified to cluster any displayed features in three dimensions: geospatial location (x, y) and color (z). This paper presents preliminary results of the clustering algorithm and cluster density calculations for a series of electronic displays with varying levels of clutter. The clutter metric correlates with preliminary, subjective clutter rankings. Our next step in validating this method will be correlating the metric with user performance.

INTRODUCTION

Objective

The objectives of this project are to develop a reliable technique for measuring clutter in navigation displays (e.g., electronic charts) and to link this clutter metric to the performance of a person using the display. The metric then could be used in the evaluation of new displays to determine the optimum amount of information that should be displayed, based on user requirements.

Background

The Navy is implementing electronic charts throughout the fleet and has already installed moving-map displays in many of its aircraft, including the F/A-18 and AV-8B. As new sources of information become available for display, and as new and innovative display techniques are developed, there is a tendency to display everything that might be of interest to the user. These new displays introduce potential human factors' issues with regard to the ability of the user to access and interpret the displayed information. Many studies have linked display complexity to user performance, especially in terms of a pilot's ability to utilize the displayed information (e.g., Aretz, 1988; Schons and Wickens, 1993; Wickens and Carswell, 1995). The last two reports found that display clutter can disrupt a pilot's visual attention, resulting in greater uncertainty concerning target locations. When a moving-map scrolls at a high rate of speed, as in the case of a large-scale cockpit display in a fighter jet, the chart's effectiveness can decrease substantially. As nautical electronic charts become more commonplace in the Navy, similar problems can be expected to arise for this user community as well.

While researchers have demonstrated a link between user performance and the presence of so-called "clutter" (which can include both the overcrowding of otherwise important information as well as unwanted data or noise), we still lack a reliable method of automatically quantifying display clutter in a way that can be empirically tied to performance.

APPROACH

Hypothesis

We theorize that our perception of clutter is primarily related to *saliency* and *color uniformity*. Saliency refers to how clearly one color or feature "pops out" from the surrounding features in an image, which we estimate by a weighted average of color gradients between adjacent features. Color uniformity refers to how closely-packed are similarly-colored pixels within the image. To discover this value, we have adapted a clustering algorithm, which we originally developed to cluster seafloor objects detected in sidescan sonar imagery. The algorithm clusters features detected within a predetermined geospatial distance from each other, produces vertices for a bounding cluster

Report Documentation Page

Form Approved
OMB No. 0704-0188

Public reporting burden for the collection of information is estimated to average 1 hour per response, including the time for reviewing instructions, searching existing data sources, gathering and maintaining the data needed, and completing and reviewing the collection of information. Send comments regarding this burden estimate or any other aspect of this collection of information, including suggestions for reducing this burden, to Washington Headquarters Services, Directorate for Information Operations and Reports, 1215 Jefferson Davis Highway, Suite 1204, Arlington VA 22202-4302. Respondents should be aware that notwithstanding any other provision of law, no person shall be subject to a penalty for failing to comply with a collection of information if it does not display a currently valid OMB control number.

1. REPORT DATE MAR 2006		2. REPORT TYPE		3. DATES COVERED 00-00-2006 to 00-00-2006	
4. TITLE AND SUBTITLE Feature Clustering to Measure Clutter in Electronic Displays				5a. CONTRACT NUMBER	
				5b. GRANT NUMBER	
				5c. PROGRAM ELEMENT NUMBER	
6. AUTHOR(S)				5d. PROJECT NUMBER	
				5e. TASK NUMBER	
				5f. WORK UNIT NUMBER	
7. PERFORMING ORGANIZATION NAME(S) AND ADDRESS(ES) Naval Research Laboratory, Code 7440.1, Stennis Space Center, MS, 39529				8. PERFORMING ORGANIZATION REPORT NUMBER	
9. SPONSORING/MONITORING AGENCY NAME(S) AND ADDRESS(ES)				10. SPONSOR/MONITOR'S ACRONYM(S)	
				11. SPONSOR/MONITOR'S REPORT NUMBER(S)	
12. DISTRIBUTION/AVAILABILITY STATEMENT Approved for public release; distribution unlimited					
13. SUPPLEMENTARY NOTES Proceedings of the Industry Engineering and Management Systems (IEMS) 2006 Conference, 13-15 Mar, Cocoa Beach, FL					
14. ABSTRACT see report					
15. SUBJECT TERMS					
16. SECURITY CLASSIFICATION OF:			17. LIMITATION OF ABSTRACT	18. NUMBER OF PAGES	19a. NAME OF RESPONSIBLE PERSON
a. REPORT	b. ABSTRACT	c. THIS PAGE			
unclassified	unclassified	unclassified	Same as Report (SAR)	8	

polygon, and calculates the cluster’s density as the number of clustered features divided by the area of the polygon. For this project, we adapted the clustering algorithm to operate in 3D space, where the third dimension is color. Our “color uniformity” value is then derived from the density of similarly-colored pixels within a 3D cluster (e.g., density = a weighted number of points within the cluster divided by the cluster’s volume).

We describe image clutter in terms of both local and global clutter components. A Local Clutter Metric (LCM) described in this paper represents the contribution of one color or feature to the overall image clutter, and equals 1 minus the weighted average (by area) of the densities of all clusters centered on that color or feature. A Global Clutter Metric (GCM) represents the overall image clutter, equal to the weighted average of the LCM’s for all colors or features in the image.

Figure 1 illustrates our proposed clutter function, in terms of saliency and LCM/GCM. The following sections describe in more detail how each of these metrics is calculated.

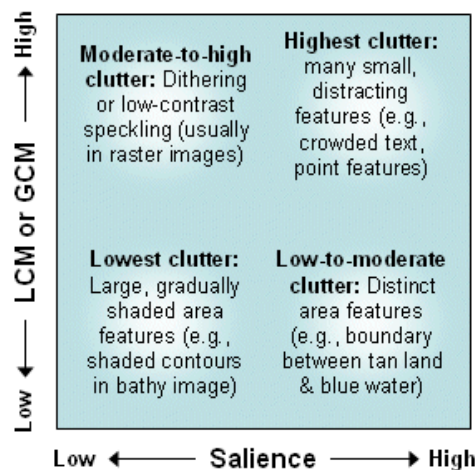


Figure 1. Clutter as a function of saliency and LCM (for local clutter) or GCM (global clutter).

3D Clustering using Geospatial Bitmaps (GB)

The original clustering algorithm relies on a geospatial bitmapping (GB) technique patented by NRL in 2001 (Gendron, et. al, 2001). The clustering algorithm itself was disclosed to the NRL Legal Office as another potential patent in June 2003. The algorithm is unique in that it is an autonomous, computationally efficient “single-pass” method and operates on a user-defined area of interest. The algorithm performs the following tasks: 1) cluster features by 2D geospatial location; 2) smooth and simplify the resultant cluster boundaries (optional); and 3) calculate a numerical measure of “cluster density,” which considers the number and size of objects clustered in a given area, as well as the scale or resolution of the complete dataset. An enhancement to the original algorithm for this project is the ability to cluster features in three or more dimensions: two geospatial (x, y) dimensions plus a third (z) dimension such as color, size, or feature type. This paper presents preliminary results of clustering by geospatial location and color.

The clustering algorithm discussed in this paper is a non-hierarchical algorithm similar to – but more efficient than – Nearest Neighbor (NN), which iteratively calculates and compares the distances between every pair of elements in the dataset to determine which elements should be clustered together. The GB algorithm is non-iterative, faster, less computationally intensive, and requires less computer memory than NN. The authors suggest that the GB algorithm is well-suited to autonomous clustering applications, because the ordering of elements input to the GB algorithm has no effect on the resulting clusters (unlike NN and other single-pass methods), and the GB algorithm does not require a seed point to initiate clustering (unlike K-means and other relocation methods).

The GB algorithm uses simple bitmaps – with a depth of one bit per pixel – which are binary structures (e.g., binary images) in which bits are turned on (set = 1) or off (cleared = 0). The index of each bit is unique and denotes its

position relative to the other bits in the bitmap. In a 2D bitmap, each bit is indexed by its column (x) and row (y); in 3D, each bit is indexed by x, y, and depth (z). A set bit indicates that an element of interest exists at that location, accurate to within the resolution of the bitmap. A cleared bit indicates the absence of any element at that location. Although a GB can be defined for an entire finite space, memory is only allocated – dynamically – when groups of spatially close bits are set, resulting in a compact data structure that supports very fast Boolean and morphological operations.

For this project, 3D bitmaps were used to cluster the pixels in an image of interest, based on geospatial location (x, y) and color (z). A separate clustering was performed for each color in the image. For example, figure 2 illustrates the results of clustering the shoreline pixels (darker brown color) in the sample image (left). All pixels within a geospatial distance of 1 (x and y) and a color distance of 9 (using the Commission Internationale d'Eclairage (CIE) L*a*b* color space) are included in the clusters, which are shown in green (right). In this case, the resulting clusters only contain the shoreline pixels themselves. If z were increased to 10, every pixel in this image would be contained in a single cluster, because every pixel in this image is immediately surrounded by pixels that are within a color distance of 10 in CIE L*a*b* space.

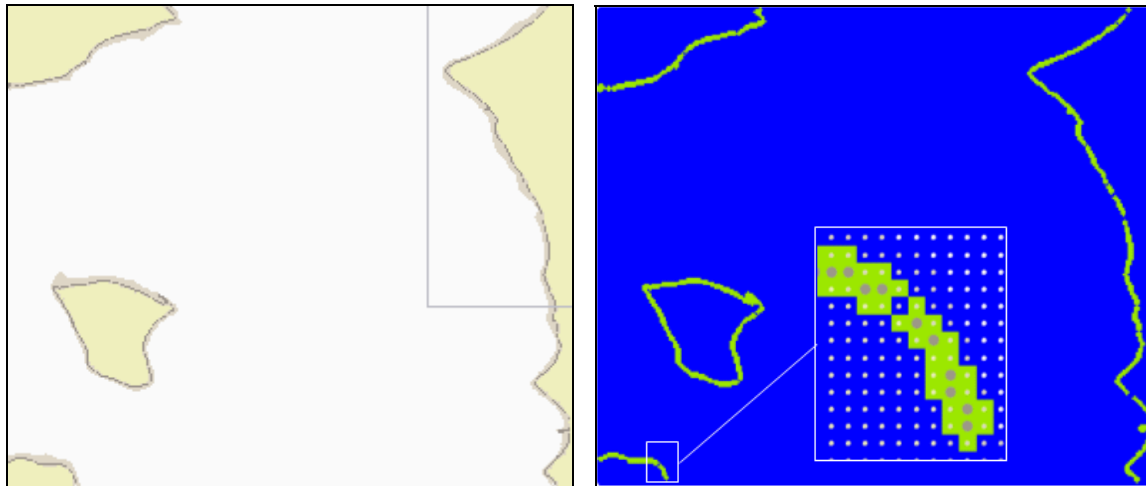


Figure 2. Example of clustering by geospatial location and color: all pixels within a predetermined distance in geospatial ($x=1$, $y=1$) and color ($z=9$) space of the shoreline pixels (brown pixels in the original image, left) are clustered together. The resulting clusters are shown in green, right. The zoomed-in section shows a detail of the pixels being clustered.

Calculating Cluster Density

After clustering all pixels in the image into bounded polygons for a given “seed color” \mathbf{s} , a cluster density \mathbf{D}_p is calculated for each cluster polygon \mathbf{p} :

$\mathbf{D}_p = \Sigma(\mathbf{W}_c \mathbf{N}_c) / \mathbf{A}_p$ where:

\mathbf{W}_c = Weighting factor for color \mathbf{c}
 $= 1 - \mathbf{E}_c / \mathbf{M}$

\mathbf{E}_c = Euclidean distance between colors \mathbf{c} and \mathbf{s} in the chosen color space; e.g., for CIE L*a*b*:
 $= \text{SQRT} [(\mathbf{L}_c - \mathbf{L}_s)^2 + (\mathbf{a}_c - \mathbf{a}_s)^2 + (\mathbf{b}_c - \mathbf{b}_s)^2]$

\mathbf{M} = Maximum distance between colors in chosen color space

\mathbf{N}_c = Number of pixels of color \mathbf{c} in the cluster polygon

\mathbf{A}_p = Area of cluster polygon \mathbf{p}

The color of each pixel in the cluster will be within a color distance of z from all immediately surrounding pixels in the cluster, starting with pixels of color \mathbf{s} . In other words, the cluster will “chain” pixels together to form the cluster, starting with each pixel of color \mathbf{s} and subsequently including all other pixels within a geospatial distance of x , y and a color distance of z . If $z = 0$, then $\mathbf{D}_p = \mathbf{N}_s / \mathbf{A}_p$.

Note the inverse relationship between clutter and “density” as it is used here: higher density tends to predict lower clutter, since density describes how closely-packed like-pixels are in the image.

Local and Global Clutter Metrics

Local density (D_S) estimates how much an individual seed color (s) contributes to the overall clutter of the image. D_S is computed as the weighted average of the densities for all clusters centered on color s :

$D_S = \Sigma(D_P A_P) / A_S$ where:

D_P = Density of cluster p (described in the previous section)

A_S = Sum of areas of all clusters for color s

Global density (D_I), which estimates clutter for the entire image, is computed as the weighted average of the local clutter densities for all colors in the image:

$D_I = \Sigma(D_S A_S) / A_I$ where:

D_S = Weighted average of clutter densities for all clusters centered on color s (described above)

A_I = Sum of all A_S 's for image i

We will refer to $(1 - D_S)$ as the Local Clutter Metric (LCM) for color s , and $(1 - D_I)$ as the Global Clutter Metric (GCM) for image i .

Saliency

We estimate the local saliency of a given color or feature as a weighted average of the color differences between each color or feature of interest and immediately adjacent colors or features. For example, if one feature in the image (e.g., a yellow lighthouse symbol on a nautical chart) is completely surrounded by another feature (e.g., solid blue water), we would estimate the saliency of the lighthouse as the Euclidean distance between these two colors (yellow and blue) in a perceptually representative color space. If this lighthouse symbol were placed on a shoreline (brown), such that 40% of the lighthouse symbol was bordered by the blue water, 40% by tan land, and 20% by the brown shoreline, we would estimate the saliency of the lighthouse by $0.4*(blue-yellow) + 0.4*(tan-yellow) + 0.2*(brown-yellow)$. Global saliency is estimated as the weighted average of the local saliencies for all colors (or features) in the image. Greater color distances result in greater saliency.

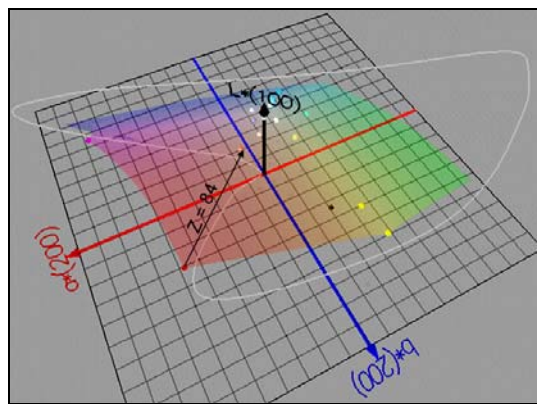


Figure 3. CIE L*a*b* color space, with colors from a sample electronic display plotted using the ColorSpace program (Colantoni, 2005).

The choice of an appropriate color space is central to this theory. Unfortunately, no single color space has been shown to perfectly model human visual perception. For this paper, we chose the CIE L*a*b* color space (pictured in figure 3), but we are continuing to search for improved options.

RESULTS

Clutter Metrics for Sample Chart Series

Figure 4a presents a sample image (a nautical chart) comprised of 9 primary features and 18 total colors. Figure 4b shows the LCM for each color component and each feature in the image. The LCM does not account for saliency, which might explain why certain features (e.g., the green feature off the northeast corner of the small island) are listed with higher clutter values than expected.

Figure 5 presents the GCM for five different charts in this nautical chart series. As more features are added to the chart, the GCM increases, indicating higher levels of clutter.

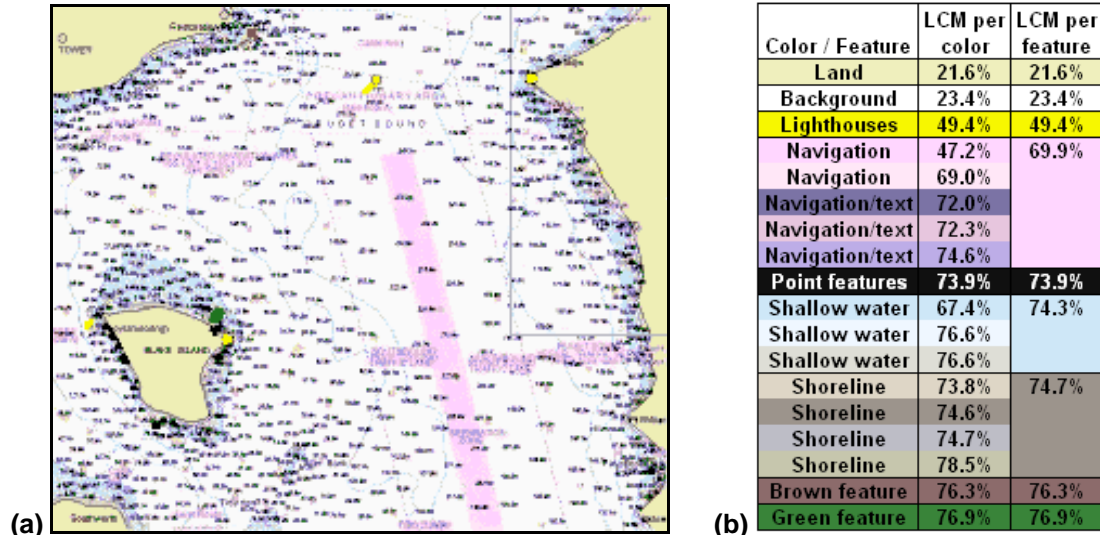


Figure 4a). Sample nautical chart comprised of 9 primary features and 18 total colors. 4b) LCM for each color and feature in the image (sorted from lowest to highest LCM). Higher LCM values indicate greater contributions to image clutter, but do not account for saliency.

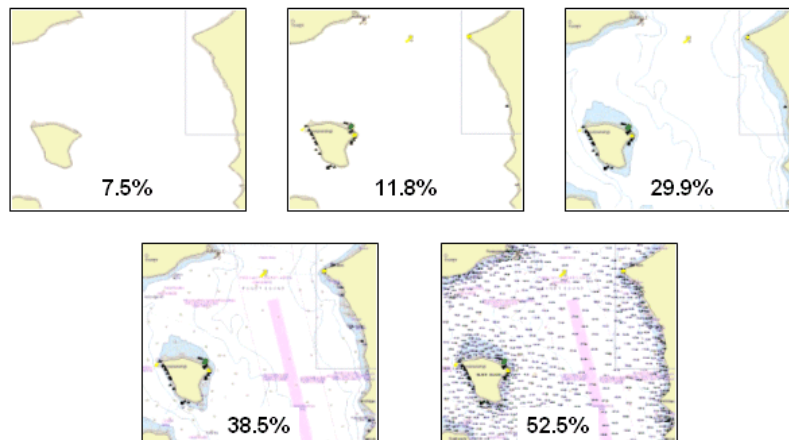


Figure 5. GCM for five charts in a nautical chart series.

Correlation between Subjective Clutter Ratings and Saliency, LCM, and GCM

As a first attempt to ascertain whether the proposed clutter metrics corresponded at all with perceived clutter (prior to receiving approval to perform human subject trials), the first author rated the individual features of several

images, to indicate how much each feature contributed clutter to the image, according to the following rudimentary rating scale:

Low clutter: feature contributes very little clutter to image

Medium clutter: feature contributes some clutter to image

High clutter: feature contributes substantial clutter to image

For 330 features rated from 28 images, the probability that a correlation between subjective ratings of local clutter and each tested clutter metric (alone) was due to chance was $p < 0.0001$ ($\chi^2 = 314.3$) for LCM, and $p < 0.0001$ ($\chi^2 = 27.9$) for saliency. An ordinal logistic fit of the ratings with a combination of both metrics was slightly more significant than with the LCM metric alone ($\chi^2 = 316.3$). Figure 6 plots local saliency figures vs. LCM, with each data point colored according to its subjective clutter rating.

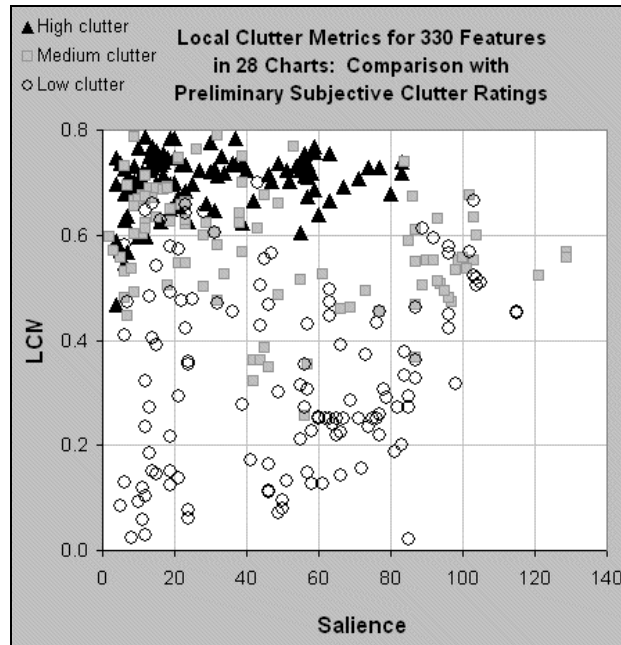


Figure 6. Comparison of subjective clutter ratings with local saliency vs. LCM.

Likewise, the author rated the images for how cluttered, overall, each appeared:

Low clutter: very easy to read image

Medium clutter: can read some information on the image; other information is hard to discern

High clutter: difficult to make sense of the image

For 28 images, the probability that a correlation between the subjective ratings of global clutter and each tested clutter metric (alone) was due to chance was $p < 0.0001$ ($\chi^2 = 25.4$) for GCM, and $p < 0.05$ ($\chi^2 = 4.1$) for saliency. An ordinal logistic fit of the subjective ratings with a combination of both metrics was more significant than with either metric alone: $p < 0.0001$ ($\chi^2 = 38.0$). Figure 7 plots global saliency figures vs. GCM, with each data point colored according to its subjective clutter rating.

Of course, with only a single subject, these results are very preliminary. A follow-on study is underway to collect subjective ratings from a larger user population for comparison with these clutter metrics.

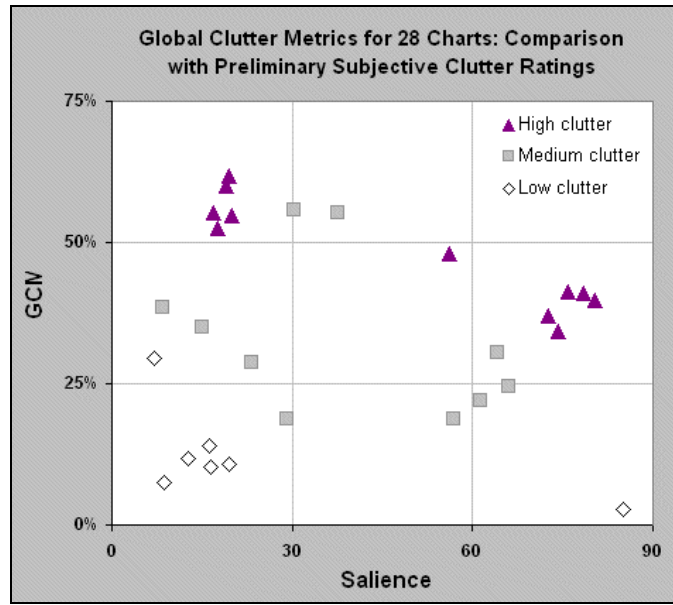


Figure 7. Comparison of subjective clutter ratings with global saliency vs. GCM.

DISCUSSION

The theory proposed at the beginning of this paper appears to have merit: a preliminary subjective evaluation of both local and global clutter seems to correlate with the LCM and GCM values, especially when saliency is considered in conjunction with these metrics. Four global clutter examples are provided in figure 8, illustrating the extremes for GCM and saliency.



Figure 7a. Low global saliency and high GCM = moderate-to-high clutter.

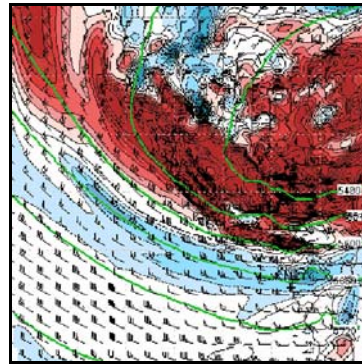


Figure 7b. High global saliency and high GCM = high clutter.



Figure 7c. Low global saliency and low GCM = low clutter.

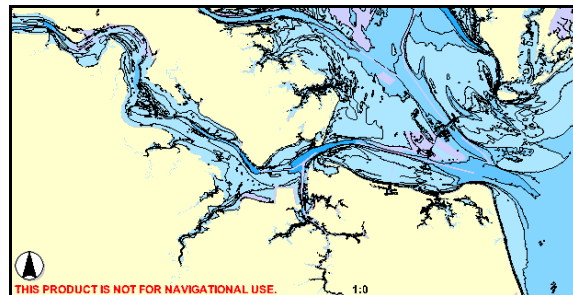


Figure 7d. High global saliency and low GCM = low-to-moderate clutter.

For example, Low GCM (i.e., high color uniformity) and low saliency tends to result in low clutter, such as in images with relatively large, uniform areas that do not contrast sharply with each other (e.g., figure 7c). Conversely, high GCM and high saliency tends to result in high clutter (e.g., figure 7b). Low saliency and high GCM tends to result in moderate-to-high clutter (e.g., figure 7a), in which the image is populated with smaller features that don't contrast well and may be difficult to discern. Finally, high saliency and low GCM results in low-to-moderate clutter, in which relatively large features contrast sharply with each other (such as the land and water areas, clearly delineated by black shoreline boundaries, in figure 7d).

The next phase of this project includes analyzing over 150 images of various types (e.g., aeronautical charts, nautical charts, topographic maps, city/road maps, weather / meteorological charts, subway maps, airport terminal maps, etc.) to correlate subjective evaluations of clutter with the GCM, LCM, and saliency metrics described in this paper. User performance studies are also planned, to determine whether these metrics can predict performance.

ACKNOWLEDGEMENTS

This work was sponsored under Program Element 002435N by the NRL 6.2 Base Program. The authors thank Stephanie Myrick, Mike Trenchard, and Dr. Greg Trafton (all of NRL) for their assistance in collecting sample charts and other images for this study. The authors are collaborating with Dr. Trafton to collect additional subjective user ratings and user performance data in support of this project.

REFERENCES

Aretz, A. (1988). A model of electronic map interpretation. In *Proceedings of the Human Factors Society 32nd Annual Meeting*, Santa Monica, CA, pp. 130-135.

Colantoni, P. (2005). *ColorSpace.exe version 1.1*, downloaded from <http://www.couleur.org>.

Gendron, M., P. Wischow, M. Trenchard, M. Lohrenz, L. Riedlinger, M. Mehaffey (2001). *Moving map composer (MMC)*. U.S. Patent #6,218,965 B1, April.

Rosenholtz, R., Y. Li, J. Mansfield, and Z. Jin (2005). Feature Congestion: A Measure of Display Clutter. *Proceedings of CHI 2005*, Portland, OR, April 2-7.

Schons, V. and C. Wickens (1993). Visual separation and information access in aircraft display layout. *University of Illinois Institution of Aviation Technical Report ARL-93-7/NASA-A3I-93-1*, Savoy, IL.

Wickens, C. and C. Carswell (1995). The proximity compatibility principle: its psychological foundation and relevance to display design. *Human Factors* 37(3), pp. 473-494.